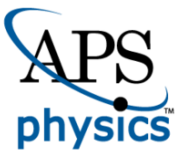

Orientational Distribution of Free O-H Groups of Interfacial Water is Exponential

Shumei Sun, Fujie Tang, Sho Imoto, Daniel R. Moberg, Tatsuhiko Ohto, Francesco Paesani, Mischa Bonn, Ellen H. G. Backus, and Yuki Nagata

Phys. Rev. Lett. **121**, 246101 — Published 10 December 2018

DOI: 10.1103/PhysRevLett.121.246101

The Orientational Distribution of Free O-H Groups of Interfacial Water Is Exponential

Shumei Sun,[1,#] Fujie Tang,[1,2,#] Sho Imoto,[1] Daniel R. Moberg,[3] Tatsuhiko Ohto,[4] Francesco Paesani,[3] Mischa Bonn,[1*] Ellen H. G. Backus,[1*] and Yuki Nagata[1*]

1. Max Planck Institute for Polymer Research, Ackermannweg 10, 55128 Mainz, Germany
2. International Center for Quantum Materials, Department of Physics, Peking University, 5 Yiheyuan Road, Haidian, Beijing 100871, China
3. Department of Chemistry and Biochemistry, University of California, San Diego, La Jolla, California 92093, United States
4. Graduate School of Engineering Science, Osaka University, 1-3 Machikaneyama, Toyonaka, Osaka 560-8531, Japan

# These authors equally contributed to this work.

*Email: nagata@mpip-mainz.mpg.de, backus@mpip-mainz.mpg.de, bonn@mpip-mainz.mpg.de

Abstract

The orientational distribution of free O-H (O-D) groups at the H_2O (D_2O)-air interface is investigated using combined molecular dynamics (MD) simulations and sum-frequency generation (SFG) experiments. The average angle of the free O-H groups, relative to the surface normal, is found to be ~63^o, substantially larger than previous estimates of 30 - 40^o. This discrepancy can be traced to erroneously assumed Gaussian/stepwise orientational distributions of free O-H groups. Instead, MD simulation and SFG measurement reveal a broad and exponentially decaying orientational distribution. The broad orientational distribution indicates the presence of the free O-H group pointing *down* to the bulk. We ascribe the origin of such free O-H groups to the presence of capillary waves on the water surface.

Main Text

At the interface of water with hydrophobic media, the hydrogen-bond (H-bond) network of water is interrupted, making the O-H groups of the topmost interfacial water molecules dangling (free) from the H-bond network. These free O-H groups are important for determining the energetics of the water surface and are thereby critical for explaining the exceptionally high surface tension of water. Furthermore, free O-H groups provide a unique platform for hydrophobic hydration assembly [1–3], on-water catalysis [4], and growth of aerosol particles [5,6]. As such, there have been many efforts to quantify the number and orientation of free O-H groups at different aqueous interfaces.

The free O-H (O-D) groups of interfacial water can be studied experimentally by a sharp peak at ~3700 (~2740) cm^{-1} in the surface-specific vibrational sum-frequency generation (SFG) spectrum [7–12]. The frequency of the free O-H signal has been examined to determine the interaction strength of the topmost water layer and the hydrophobic medium [13–17]. Moreover, the free O-H SFG response measured with different polarization combinations provides information about their orientation. From the *ssp*-SFG (shorthand for *s*, *s,* and *p* polarized sum-frequency output, visible input, and infrared input, respectively) and *ppp*-SFG signals of the free O-H stretch, the averaged angle of the free O-H group at the water-air interface has previously been estimated to 30-40^{o} [17–19]. The orientational distribution of the free O-H group has been concluded to broaden with increasing temperature induced by disordering of the topmost water layer [20,21]. However, to connect the *ppp*-/*ssp*-SFG peak amplitudes of the free O-H stretch (A_{ppp} and A_{ssp}, respectively) with the averaged angle of the free O-H group, one needs to assume a functional form for the orientational distribution of the free O-H groups. So far, the distribution has been assumed to be stepwise shaped [18,20,21] or Gaussian shaped [17,19].

Recently, we have developed a geometrical definition of the free O-H group [22] and, based on this definition, we computed the orientation of the free O-H group from molecular dynamics (MD) simulations with the POLI2VS model [23]. Surprisingly, these simulations predict an average angle formed by the free O-H group and the surface normal to be ~63^{o} [22], much larger than the previously estimated values of 30-40^{o} [17–19]. This discrepancy casts doubts on either the quality of the water force field model or the assumption of the Gaussian/stepwise shaped orientational distribution of the free O-H groups.

Here, by combining simulation and experiment, we unveil the orientational distribution of the free O-H group at the water-air interface. We compare the results of MD simulations with various force field models, which commonly predict an average angle of ~63 ± 3^{o}. Furthermore, these results suggest that the orientational distribution of the free O-H group cannot be accurately represented by a narrow Gaussian or stepwise shaped distribution. Rather, the distribution is exponentially shaped. The combination of a large average orientation angle and an exponentially shaped distribution fully accounts for the experimental data. We discuss the sensitivity of the free O-H SFG feature to the average angle and present a physical argument for the existence of a broad orientational distribution.

We performed MD simulations of the water/air interface to characterize the structure of the free O-H group for various force field models. To define the free O-H group, we used the free O-H group definition developed recently in Ref. [22]. According to this definition, an O-H group of water is free of hydrogen bonds when the intermolecular O…O distance is larger than 3.5 Å, and the H-O…O angle is larger than 50^{o}. We used fixed-charge force field models (TIP3P, [24] TIP4P, [24] TIP4/2005, [25] TIP4P/Ew [26], TIP4P/ice [27],

SPC [28], SPC/E [29], and SPC/Fw [30]), a polarizable model (POLI2VS [23]), and a many-body model (MB-pol [31–33]). Simulation details can be found in Supplementary Materials.

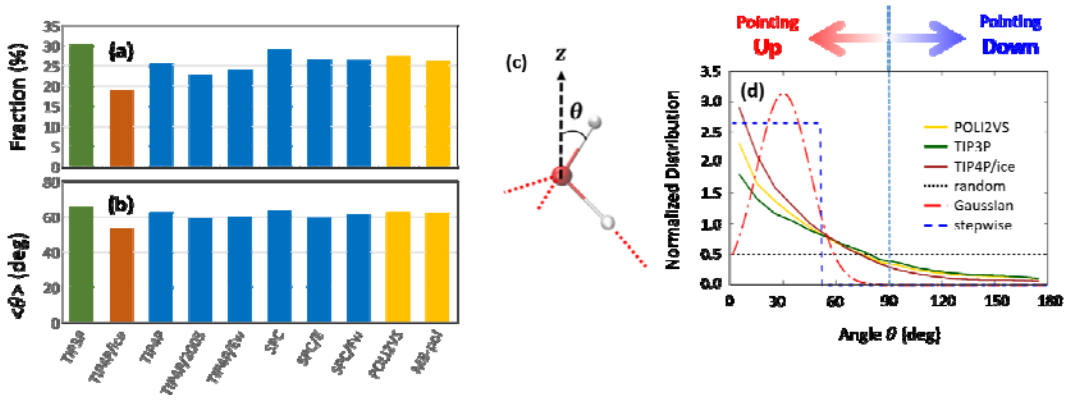

Figure 1. (a) Fractions of the water molecules with free O-H groups, and (b) average angles , computed from the MD simulations with various force field models. (c) Definition of the angle formed by the free O-H group and the macroscopic surface normal. (d) Normalized probability distributions of obtained from the POLI2VS, TIP3P and TIP4P/ice MD simulations as well as the stepwise function with [18], and the Gaussian function with and [19].

Figure 1(a) shows the simulated fraction of the interfacial water molecules with free O-H groups. The procedure for calculating the fraction of the free O-H groups is detailed in Supplementary Materials. The TIP4P/ice model provides the lowest fraction (~20 %), while the TIP3P model provides the highest fraction (~30 %). Since the TIP4P/ice model is parameterized to reproduce the properties of ice [27], it tends to overestimate the strengths of the H-bonds of water, decreasing the fraction of free O-H groups at the interface. In

contrast, the TIP3P model is known to predict extremely short H-bond lifetime [30], indicating that the strength of the H-bonds in the TIP3P model is weaker than in the other water force field models. Thus, the TIP3P model predicts the highest fraction of the free O-H group. The fractions of the free O-H group for various force field models are 25 ± 5 %, which is consistent with experimental data [34].

Figure 1(b) displays the average angle $\langle\theta\rangle$ formed by the free O-H groups and the surface normal (see Figure 1(c)), where the thermal average of quantity A is calculated as $\langle A\rangle = \int_0^\pi Af(\theta)\sin\theta\, d\theta$ and $f(\theta)$ is the orientational distribution of the free O-H groups. Again, the TIP4P/ice and TIP3P models provide the lower and upper limits, respectively, among all models considered in this study. $\langle\theta\rangle$ of the free O-H groups is 59 - 66°. This is, however, in stark contrast with the previously reported values of 33.5° in Ref. [18] and 36.6° in Ref. [19].

These values of 33.5° and 36.6° were obtained from a comparison of *ssp*- and *ppp*-SFG intensity measurements in the following way. From the measured SFG intensity in *ssp* and *ppp* polarizations (proportional to $|\chi_{ssp}^{(2),\mathrm{eff}}|^2$ and $|\chi_{ppp}^{(2),\mathrm{eff}}|^2$, respectively), $\chi_{xxz}^{(2)} = \chi_{yyz}^{(2)}$ and $\chi_{zzz}^{(2)}$ are obtained via:

$$\chi_{ssp}^{(2),\mathrm{eff}} = L_{yy}(\omega)L_{yy}(\omega_1)L_{zz}(\omega_2)\,\sin\beta_2\,\chi_{yyz}^{(2)} \quad (1)$$

$$\chi_{ppp}^{(2),\mathrm{eff}} \approx -L_{xx}(\omega)L_{xx}(\omega_1)L_{zz}(\omega_2)\cos\beta\cos\beta_1\sin\beta_2\chi_{xxz}^{(2)}$$

$$+L_{zz}(\omega)L_{zz}(\omega_1)L_{zz}(\omega_2)\sin\beta\sin\beta_1\sin\beta_2\chi_{zzz}^{(2)} \quad (2)$$

where L_{ii} $(i = x, y, z)$ is the Fresnel Factor and β_i is the incidence/reflection angle of the light of frequency ω_i with respect to the surface normal. Here, the *x*-*y* plane is defined

parallel to the surface and the *z*-axis forms the macroscopic surface normal. The amplitudes of the free O-H peak A_{xxz} and A_{zzz} in the $\chi^{(2)}_{xxz}$ and $\chi^{(2)}_{zzz}$ spectra, respectively, are related to $\langle\cos^3\theta\rangle/\langle\cos\theta\rangle$ via:

$$\frac{A_{xxz}}{A_{zzz}} \propto \frac{(1+r)\langle\cos\theta\rangle - (1-r)\langle\cos^3\theta\rangle}{2r\langle\cos\theta\rangle + 2(1-r)\langle\cos^3\theta\rangle} \tag{3}$$

in the slow motion limit [18], and is linked to $\langle\cos^2\theta\rangle$ via:

$$\frac{A_{xxz}}{A_{zzz}} \propto \frac{(1+r) - (1-r)\langle\cos^2\theta\rangle}{2r + 2(1-r)\langle\cos^2\theta\rangle} \tag{4}$$

in the fast motion limit [19]. For the slow (fast) motion limit, the decay of the orientational memory of the free O-H group is much slower (faster) than vibrational relaxation. *r* is given by the ratio of the transition polarizability $\dot{\alpha}_{\zeta\zeta}/\dot{\alpha}_{\xi\xi}$, where ξ and ζ denote the directions parallel to and perpendicular to the O-H bond, respectively (see Supplementary Materials). To obtain the average angle $\langle\theta\rangle$ from $\langle\cos^3\theta\rangle/\langle\cos\theta\rangle$ or $\langle\cos^2\theta\rangle$, one needs to assume an orientational distribution. Previously, a stepwise function [18,20,21]:

$$f(\theta) = \begin{cases} N_S \text{ for } 0 \le \theta \le \theta_S \\ 0 \text{ for } \theta_S < \theta < \pi \end{cases}, \tag{5}$$

and Gaussian function [17,19]:

$$f(\theta) = \frac{N_G}{\sqrt{2\pi\sigma^2}} \mathrm{e}^{-(\theta-\theta_G)^2/2\sigma^2}, \tag{6}$$

have been used, where N_S and N_G are determined from the normalization condition;

$$\int_0^\pi f(\theta)\sin\theta\, d\theta = 1. \tag{7}$$

Since the discrepancy between $\langle\theta\rangle$ = 63° in the simulation [22] and ~35° deduced from the experiments [18,19] may arise from the improperly assumed orientational

distributions, we calculated the angular distributions from the MD simulations. These are displayed in Figure 1(d). The shapes of the computed distributions are very similar for different force field models, but differ significantly from the narrow Gaussian/stepwise shaped distributions. We find that the simulated distributions can be described well by an exponential curve:

$$f(\theta) = N_E \mathrm{e}^{-\theta/\theta_E}, \quad (8)$$

where N_E is the normalization parameter satisfying Eq. (7). For the POLI2VS model, θ_E = 53.3°. This illustrates that the Gaussian/stepwise shaped distributions are not appropriate for describing the free O-H group orientation at the water-air interface.

To examine whether this broad, exponentially decaying distribution of free O-H angles is consistent with the experimental data, we carried out SFG measurements with *ssp*- and *ppp*-polarization combinations at the D_2O-air interface. Since the *ppp*-SFG signal is sensitive to the experimental setup geometry, we used two experimental geometries to verify that the ratio of the amplitude for the free O-D group (A_{xxz}/A_{zzz}) is robust. In the experimental geometry 1, the incident angles of IR and visible are 62° and 47°, respectively, while in geometry 2, the incident angles of IR and visible are 40° and 56°, respectively. The SFG intensity data are plotted in Figure 2(a) and (d), respectively. By fitting the intensity spectra (parameters are listed in Supplementary Materials), we obtained $\mathrm{Im}\left(\chi_{ssp}^{(2),\mathrm{eff}}\right)$ and $\mathrm{Im}\left(\chi_{ppp}^{(2),\mathrm{eff}}\right)$. These are plotted in Figure 2(b) and (e) for geometry 1 and 2, respectively. Furthermore, we obtained $\mathrm{Im}\left(\chi_{xxz}^{(2)}\right)$ and $\mathrm{Im}\left(\chi_{zzz}^{(2)}\right)$ from $\mathrm{Im}\left(\chi_{ssp}^{(2),\mathrm{eff}}\right)$ and $\mathrm{Im}\left(\chi_{ppp}^{(2),\mathrm{eff}}\right)$ via Eqs. (1) and (2), where the calculation of Fresnel factors is detailed in Supplementary Materials. These are displayed in Figure 2(c) and (f) for geometry 1 and 2, respectively.

$\mathrm{Im}\left(\chi_{xxz}^{(2)}\right)$ and $\mathrm{Im}\left(\chi_{zzz}^{(2)}\right)$ spectra show that the two data sets of the different incident angles are in good agreement. From these spectra, we obtain a ratio of A_{xxz}/A_{zzz} of 0.43 ± 0.02 (geometry 1: 0.45, geometry 2: 0.42, see Sec. III. C of Supplementary Materials). Furthermore, as is seen in Figure 2(c) and (f), the simulated $\mathrm{Im}\left(\chi_{xxz}^{(2)}\right)$ and $\mathrm{Im}\left(\chi_{zzz}^{(2)}\right)$ data with the POLI2VS model [23] are also in good agreement with the experimental data.

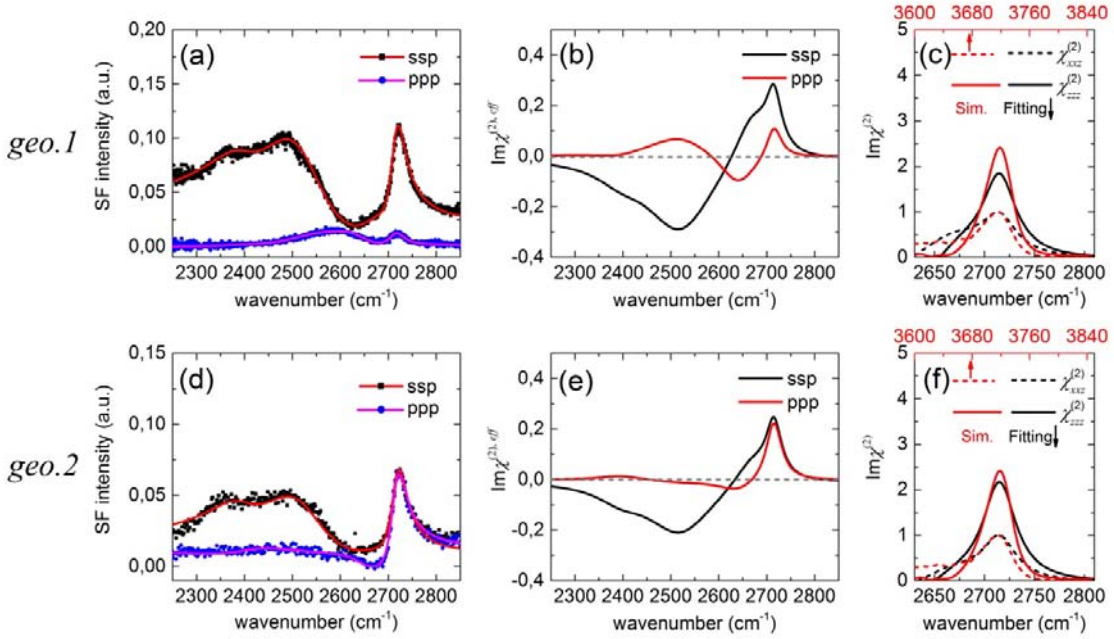

Figure 2. (a) *ssp*- and *ppp*-SFG intensity spectra of D_2O at the D_2O-air interface, (b) imaginary part of the effective spectra containing the Fresnel factors; $\mathrm{Im}\left(\chi_{ssp}^{(2),\mathrm{eff}}\right)$ and $\mathrm{Im}\left(\chi_{ppp}^{(2),\mathrm{eff}}\right)$ obtained from the fit of the intensity spectra, (c) $\mathrm{Im}\left(\chi_{xxz}^{(2)}\right)$ and $\mathrm{Im}\left(\chi_{zzz}^{(2)}\right)$ constructed from $\mathrm{Im}\left(\chi_{ssp}^{(2),\mathrm{eff}}\right)$ and $\mathrm{Im}\left(\chi_{ppp}^{(2),\mathrm{eff}}\right)$ for experimental geometry 1, and (d) *ssp*- and *ppp*-SFG intensity spectra (e) $\mathrm{Im}\left(\chi_{ssp}^{(2),\mathrm{eff}}\right)$ and $\mathrm{Im}\left(\chi_{ppp}^{(2),\mathrm{eff}}\right)$, (f) $\mathrm{Im}\left(\chi_{xxz}^{(2)}\right)$ and $\mathrm{Im}\left(\chi_{zzz}^{(2)}\right)$ for experimental geometry 2. In (a) and (d), the fit data is also shown. In (c) and (f), simulated

data for H_2O with the POLI2VS model is also shown. and in (c) and (f) were normalized, based on the free O-D peak amplitude in .

The experimentally obtained = 0.43 ± 0.02 can now be compared with the simulation data. To do so, we calculated the variation of as a function of for the exponential shaped distribution (Eq. (8)), by using Eqs. (3) and (4) with r = 0.15. Although this r was set to 0.32 in Ref. [35], we used r = 0.15 obtained from *ab initio* calculation of water trimer at the B3LYP/aug-cc-pVTZ level of theory (see Supplementary Materials). The data is shown in Figure 3(a). = 63 ± 3° provides the value of 0.42 ± 0.01 for the slow motion limit and 0.80 ± 0.04 for the fast motion limit. The value of 0.42 for the slow motion limit together with the exponential shaped distribution is consistent with the experimental result of 0.43 ± 0.02, manifesting that a broad exponentially shaped distribution and the expression of the slow motion limit (Eq. (8)) can indeed account for the experimental data.

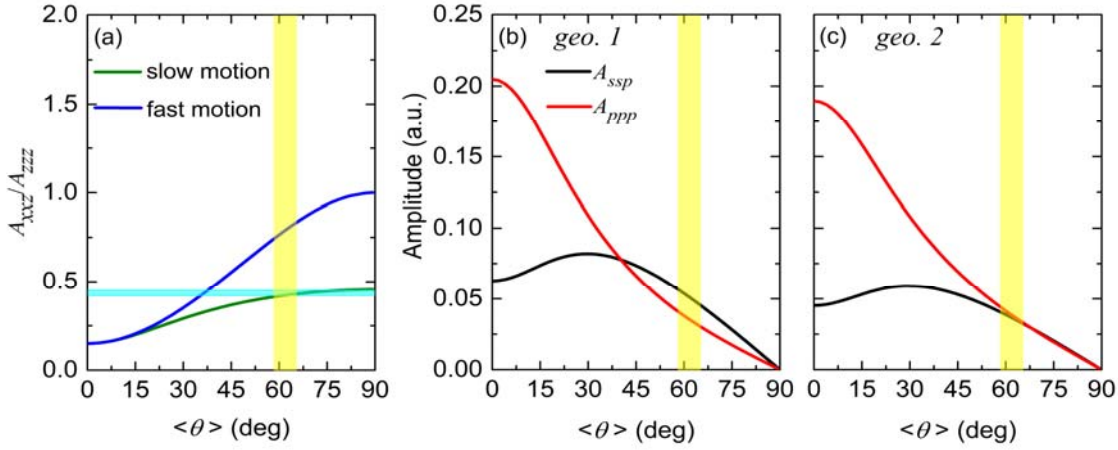

Figure 3. (a) Variations of A_{xxz}/A_{zzz} as a function of average angle <θ> computed based on the exponential distribution represented by Eq. (8). The sky blue zone represents the experiment tolerance and the yellow zone represents the simulation tolerance. A_{ssp} and A_{ppp} vs. <θ> based on the slow motion approximation and exponential shaped orientational distribution for (b) experimental setup geometry 1 and (c) geometry 2.

The broad exponentially shaped distribution has two important consequences. One is that both the *ssp*- and *ppp*-SFG amplitudes of the free O-H (O-D) stretch (A_{ssp} and A_{ppp}, respectively) are very sensitive to the average angle of the free O-H group around 63° as is seen in Figure 3(b) and (c). This observation contrasts the previous conclusion that *ssp*-signals would be insensitive to the angle of the free O-H group [18,20,21]. Our finding indicates that the variation of A_{ssp} cannot be solely attributed to the variation of the number of free O-H (O-D) stretch chromophores when the average angle is larger than 50°. This can resolve the apparent contradiction on the surface activity of small osmolyte molecules at the water-air interface: the absence of the osmolyte in the topmost water layer has been concluded from the insensitivity of the free O-H stretch *ssp*-SFG peak to the addition of osmolyte [36,37], while MD simulations have suggested that osmolyte molecules should be located at the topmost water layer [38,39]. Since the average angle of the free O-H group changes due to the addition of osmolyte, the reduction of the free O-H stretch chromophores is compensated by the decrease in $\langle\theta\rangle$ (increase in $\langle\cos\theta\rangle$), yielding no overall change in the SFG peak amplitude [40]. Hence, the SFG intensity remains constant due to a cancellation of counteracting effects. The appearance of TMAO at the topmost water layer demonstrates that the methyl group of TMAO is very hydrophobic, which is critical to

account for the counteracting effects of TMAO and urea on the protein folding. [41,42] Furthermore, this work suggests that the orientational distribution should be carefully examined to obtain the average angles not only for the O-H stretch mode of water but also for the C=O, N-H and C-H stretch mode. These modes have been frequently used for probing proteins [43,44], a small molecule [45], and lipids [46,47] at the water-air interface as well as the ionic liquid-air interface [48–51].

The other consequence is that for the broad exponential distribution with θ_E = 53.3^o in Eq. (8), ~20 % of the free O-H groups at the water-air interface point *down* to the bulk, unlike the narrow Gaussian/stepwise shaped distributions. In fact, a free O-H group pointing *down* has not been recognized [52]. The mechanism of the presence of free O-H group pointing down can be understood by considering capillary waves causing surface roughness. On the top and bottom of the capillary wave, *i.e.,* the location where the gradient of the capillary wave is small, a free O-H group rarely points *down* to the bulk. In contrast, on the slope of the capillary wave, *i.e.,* the location where the gradient is very large, a free O-H group often points *down* to the bulk. This is schematically shown in Figure 4(a). A water molecule with a free O-H group pointing *down* to the bulk can be often found on the slope of the capillary wave, as apparent from the simulation snapshot shown in Figure 4(b). When we reduce the effects of the surface roughness on the angular distribution by using the instantaneous liquid interface [53], the free O-H group orientation distribution becomes narrower (see Figure S5). This clearly demonstrates that interfacial molecular orientation is assisted by capillary waves.

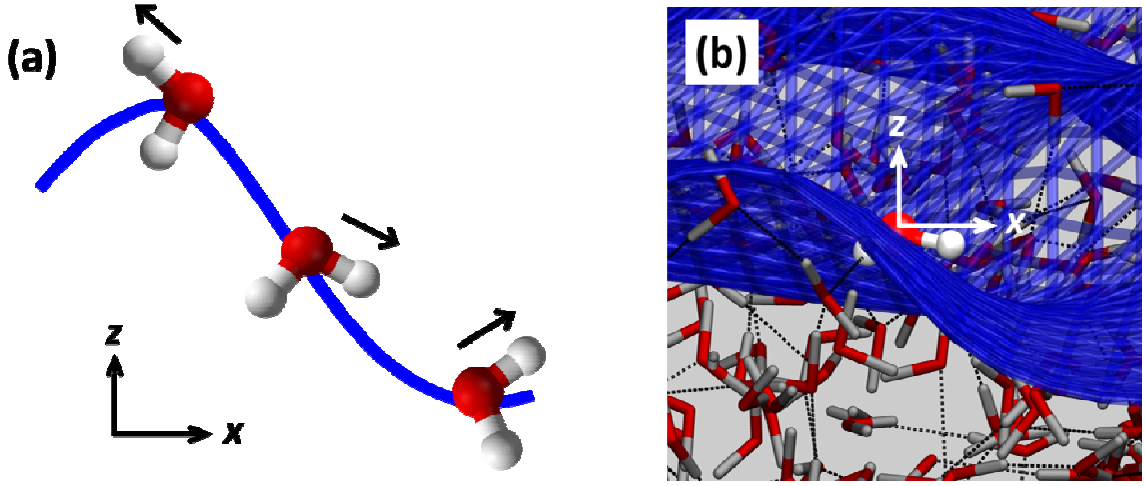

Figure 4 (a) Schematic of the interfacial water molecules. The blue line represents the capillary wave, and the black arrows denote the orientation of the free O-H group. (b) Snapshot of the simulated water-air interface. A water molecule with the free O-H group is highlighted with spheres for atoms. The black broken lines represent the hydrogen bonds, and the blue lines represent the positions of the capillary wave.

In conclusion, by combining SFG experiment and MD simulations, we examined the orientational distribution of the free O-H group at the water-air interface. The different force field models provide the average angle of the free O-H group of ~63^{o}, substantially larger than previous estimates of 30-40^{o} [17–19]. The underestimation of the angle for the previous studies arises from the assumed shape of the orientational distributions; the actual distribution of the free O-H orientation is much broader and exponentially shaped. This leads to a high sensitivity of the SFG amplitude of the free O-H stretch mode at the *ssp* polarization combination to the angle of the free O-H group, opposed to the commonly claimed insensitivity of the *ssp*-SFG signal to the angle. Furthermore, a broad distribution

indicates that ~20 % of the free O-H groups point down to the bulk. We attribute this to the free O-H groups on the slope of a capillary wave.

Acknowledgment

This work was partly funded by an ERC Starting Grant (Grant No. 336679) and a DFG grant (no. BA 5008/3). D.R.M. and F.P. were supported by the National Science Foundation (Grant. No. CHE-1453204) and used computational resources of the Extreme Science and Engineering Discovery Environment (XSEDE), which is supported by the National Science Foundation (Grant No. ACI-1053575).

References:

[1] Y. Jung and R. A. Marcus, J. Am. Chem. Soc. **129**, 5492 (2007).

[2] D. Chandler, Nature **437**, 640 (2005).

[3] S. Narayan, J. Muldoon, M. G. Finn, V. V. Fokin, H. C. Kolb, and K. B. Sharpless, Angew. Chemie - Int. Ed. **44**, 3275 (2005).

[4] B. Braunschweig, S. Eissner, and W. Daum, J. Phys. Chem. C **3**, 1751 (2008).

[5] J. Julin, M. Shiraiwa, R. E. H. Miles, J. P. Reid, U. Pöschl, and I. Riipinen, J. Phys. Chem. A **117**, 410 (2013).

[6] J. F. Davies, R. E. H. Miles, A. E. Haddrell, and J. P. Reid, Proc. Natl. Acad. Sci. U. S. A. **110**, 8807 (2013).

[7] J. A. McGuire and Y. R. Shen, Science **313**, 1945 (2006).

[8] I. V. Stiopkin, C. Weeraman, P. A. Pieniazek, F. Y. Shalhout, J. L. Skinner, and A. V. Benderskii, Nature **474**, 192 (2011).

[9] A. M. Jubb, W. Hua, and H. C. Allen, Annu. Rev. Phys. Chem. **63**, 107 (2012).

[10] C.-S. Tian and Y. R. Shen, J. Am. Chem. Soc. **131**, 2790 (2009).

[11] S. Nihonyanagi, S. Yamaguchi, and T. Tahara, J. Chem. Phys. **130**, 204704 (2009).

[12] S. Yamaguchi, J. Chem. Phys. **143**, 034202 (2015).

[13] L. F. Scatena, M. G. Brown, and G. L. Richmond, Science. **292**, 908 (2001).

[14] F. G. Moore and G. L. Richmond, Acc. Chem. Res. **41**, 739 (2008).

[15] C. S. Tian and Y. R. Shen, Proc. Natl. Acad. Sci. U. S. A. **106**, 15148 (2009).

[16] R. Vaécha, S. W. Rick, P. Jungwirth, A. G. F. De Beer, H. B. De Aguiar, J. S. Samson, and S. Roke, J. Am. Chem. Soc. **133**, 10204 (2011).

[17] R.-R. Feng, Y. Guo, and H.-F. Wang, J. Chem. Phys. **141**, 18C507 (2014).

[18] X. Wei and Y. R. Shen, Phys. Rev. Lett. **86**, 4799 (2001).

[19] W. Gan, D. Wu, Z. Zhang, R. R. Feng, and H. F. Wang, J. Chem. Phys. **124**, 114705 (2006).

[20] X. Wei, P. B. Miranda, and Y. R. Shen, Phys. Rev. Lett. **86**, 1554 (2001).

[21] X. Wei, P.B. Miranda, C. Zhang, and Y.R. Shen, Phys. Rev. B **66**, 085401 (2002).

[22] F. Tang, T. Ohto, T. Hasegawa, W. J. Xie, L. Xu, M. Bonn, and Y. Nagata, J. Chem.

Theory Comput. **14**, 357 (2018).

[23] T. Hasegawa and Y. Tanimura, J. Phys. Chem. B **115**, 5545 (2011).

[24] W. L. Jorgensen, J. Chandrasekhar, J. D. Madura, R. W. Impey, and M. L. Klein, J. Chem. Phys. **79**, 926 (1983).

[25] J. L. F. Abascal and C. Vega, J. Chem. Phys. **123**, 234505 (2005).

[26] H. W. Horn, W. C. Swope, J. W. Pitera, J. D. Madura, T. J. Dick, G. L. Hura, and T. Head-Gordon, J. Chem. Phys. **120**, 9665 (2004).

[27] J. L. F. Abascal, E. Sanz, R. García Fernández, and C. Vega, J. Chem. Phys. **122**, 234511 (2005).

[28] H. J. C. Berendsen, J. P. M. Postma, W. F. van Gunsteren, and J. Hermans, *In Intermolecular Forces: Proceedings of the Fourteenth Jerusalem Sympo- Sium on Quantum Chemistry and Biochemistry Held in Jerusalem, Israel, April 13–16, 1981, Edited by B. Pullman* (1981).

[29] H. J. C. Berendsen, J. R. Grigera, and T. P. Straatsma, J. Phys. Chem. **91**, 6269 (1987).

[30] Y. Wu, H. L. Tepper, and G. A. Voth, J. Chem. Phys. **124**, 024503 (2006).

[31] V. Babin, C. Leforestier, and F. Paesani, J. Chem. Theory Comput. **9**, 5395 (2013).

[32] V. Babin, G. R. Medders, and F. Paesani, J. Chem. Theory Comput. **10**, 1599 (2014).

[33] G. R. Medders, V. Babin, and F. Paesani, J. Chem. Theory Comput. **10**, 2906 (2014).

[34] Q. Du, E. Freysz, and Y. R. Shen, Science **264**, 826 (1994).

[35] Q. Du, R. Superfine, E. Freysz, and Y. R. Shen, Phys. Rev. Lett. **70**, 2313 (1993).

[36] M. Ahmed, V. Namboodiri, P. Mathi, A. K. Singh, and J. A. Mondal, J. Phys. Chem. C **120**, 10252 (2016).

[37] J. A. Mondal, J. Phys. Chem. Lett. **7**, 1704 (2016).

[38] A. Fiore, V. Venkateshwaran, and S. Garde, Langmuir **29**, 8017 (2013).

[39] T. Ohto, J. Hunger, E. Backus, W. Mizukami, M. Bonn, and Y. Nagata, Phys. Chem. Chem. Phys. **19**, 6909 (2017).

[40] T. Ohto, E. H. G. Backus, W. Mizukami, J. Hunger, M. Bonn, and Y. Nagata, J. Phys. Chem. C **120**, 17435 (2016).

[41] S. Paul and G. N. Patey, J. Am. Chem. Soc. **129**, 4476 (2007).

[42] W. J. Xie, S. Cha, T. Ohto, W. Mizukami, Y. Mao, M. Wagner, M. Bonn, J. Hunger, and Y. Nagata, Chem **4**, 2615 (2018).

[43] J. Wang, S. H. Lee, and Z. Chen, J. Phys. Chem. B **112**, 2281 (2008).

[44] S. Ham, J. H. Kim, H. Lee, and M. Cho, J. Chem. Phys. **118**, 3491 (2003).

[45] D. Simonelli and M. J. Shultz, J. Chem. Phys. **112**, 6804 (2000).

[46] N. Takeshita, M. Okuno, and T. A. Ishibashi, Phys. Chem. Chem. Phys. **19**, 2060 (2017).

[47] G. Ma and H. C. Allen, Langmuir **22**, 5341 (2006).

[48] C. Peñalber-Johnstone, G. Adamová, N. V. Plechkova, M. Bahrami, T. Ghaed-Sharaf, M. H. Ghatee, K. R. Seddon, and S. Baldelli, J. Chem. Phys. **148**, 193841 (2018).

[49] C. Aliaga and S. Baldelli, J. Phys. Chem. B **111**, 9733 (2007).

[50] T. Iwahashi, T. Miyamae, K. Kanai, K. Seki, D. Kim, and Y. Ouchi, J. Phys. Chem. B **112**, 11936 (2008).

[51] Y. Jeon, J. Sung, W. Bu, D. Vaknin, Y. Ouchi, and D. Kim, J. Phys. Chem. C **112**, 19649 (2008).

[52] J. N. Israelachvili, *Intermolecular and Surface Forces* (Academic press, 2011).

[53] A. P. Willard and D. Chandler, J. Phys. Chem. B 114, 1954 (2010).

[54] See Supplemental Material for simulation and experimental protocols and additional simulation and SFG data, which includes Refs. [55-70].

[55] J. Schaefer, E. H. G. Backus, Y. Nagata, and M. Bonn, J. Phys. Chem. Lett. **7**, 4591 (2016).

[56] The CP2K developer groups, http://www.cp2k.org.

[57] R. R. Khatib, T. Hasegawa, M. Sulpizi, E. H. G. Backus, M. Bonn, and Y. Nagata, J. Phys. Chem. C **120**, 18665 (2016).

[58] A. D. Becke, J. Chem. Phys. **98**, 5648 (1993).

[59] G. W. Trucks, J. A. Pople, and M. Head-Gordon, Chem. Phys. Lett. **157**, 479 (1989).

[60] F. Neese, Wiley Interdiscip. Rev. Comput. Mol. Sci. **2**, 73 (2012).

[61] A. L. Hickey and C. N. Rowley, J. Phys. Chem. A **118**, 3678 (2014).

[62] H. Li and J. H. Jensen, Theor. Chem. Acc. **107**, 211 (2002).

[63] X. Wei, S.-C. Hong, X. Zhuang, T. Goto, and Y. R. Shen, Phys. Rev. E **62**, 5160 (2000).

1 [64] W. F. Murphy, Mol. Phys. 36, 727 (1978).

2 [65] G. Avila, J. M. Fernández, G. Tejeda, and S. Montero, J. Mol. Spectrosc. 228, 38 (2004).

3 [66] X. Zhuang, P. B. Miranda, D. Kim, and Y. R. Shen, Phys. Rev. B 59, 12632 (1999).

4 [67] J. E. Bertie, M. K. Ahmed, and H. H. Eysel, J. Phys. Chem. 93, 2210 (1989).

5 [68] B. Dünweg and K. Kremer, J. Chem. Phys. 99, 6983 (1993).

6 [69] F. Sedlmeier, D. Horinek, and R. R. Netz, Phys. Rev. Lett. 103, 136102 (2009).

7 [70] F. Schmitz, P. Virnau, and K. Binder, Phys. Rev. Lett. 112, 125701 (2013).

8